

## Article

# Effect of Molecular Weight on Tribological Properties of Polyether Amine Derivatives under Different Contact Modes

Wenjing Hu and Jiusheng Li \* 

Laboratory for Advanced Lubricating Materials, Shanghai Advanced Research Institute, Chinese Academy of Sciences, Shanghai 201210, China; huwj@sari.ac.cn

\* Correspondence: lij@sari.ac.cn

**Abstract:** The requirements for the fuel economy of modern industry continue to drive the progress of low-viscosity lubricants. The present work reports the application of polyether amine derivatives as friction modifiers to improve the tribological properties of low viscosity poly-alpha-olefin. Three polyether amine derivatives with different molecular weights were synthesized, the tribological properties of which were systematically investigated under three different contact modes. These functionalized polymers exhibited significant friction reduction and wear resistance properties in the point-on-flat and line-on-flat friction tests, but just showed anti-wear performance in the severe point-to-point contact mode. The results exhibited that molecular weights of the polymers had a direct effect on their tribological properties. The increase of molecular weight in a certain range was beneficial to the improvement of tribological properties, but further undue increase will rather reduce the friction reduction and wear resistance performances. It can be indicated that the number of oxygen atoms increased with the molecular weight of the polymer, which will be conducive to the adsorption of the polymer on the metal surface. However, when the molecular weight of the polymer exceeds a certain value, the steric hindrance of the molecules adsorbing to the metal surface increases, which in turn has a negative impact on the tribological properties.

**Keywords:** polyether amine derivatives; molecular weight; friction modifier; tribological properties; contact modes



**Citation:** Hu, W.; Li, J. Effect of Molecular Weight on Tribological Properties of Polyether Amine Derivatives under Different Contact Modes. *Lubricants* **2022**, *10*, 105.

<https://doi.org/10.3390/lubricants10060105>

Received: 21 April 2022

Accepted: 25 May 2022

Published: 27 May 2022

**Publisher's Note:** MDPI stays neutral with regard to jurisdictional claims in published maps and institutional affiliations.



**Copyright:** © 2022 by the authors. Licensee MDPI, Basel, Switzerland. This article is an open access article distributed under the terms and conditions of the Creative Commons Attribution (CC BY) license (<https://creativecommons.org/licenses/by/4.0/>).

## 1. Introduction

The rapid growth of the automobile industry has led to excessive energy consumption and environmental pollution [1,2]. Increasingly strengthened environmental regulations continue to promote the creation of ways to reduce friction and wear between engine components [3]. In order to maximize fuel economy during engine operation, the technology of low viscosity lubricants has been extensively improved [4–7]. However, the reduction of viscosity will reduce the oil film thickness, and it will make the oil film discontinuous in all conditions, but certainly in more cases than a higher viscosity oil. Low viscosity engine oil makes the engine parts operate frequently in a mixed lubrication or boundary lubrication regime, in which most of the oil film will be extruded from the interfaces. Thus, low viscosity engine oil requires a layer of protective film which can separate the sliding surfaces to reduce friction and wear. For that, friction modifiers (FMs) are deployed on the friction interfaces to form densely arranged adsorption or tribochemical films [8,9].

The modern automobile industry's demand for fuel economy continuously drives the development of FMs. According to the molecular structure characteristics, FMs include the following types: organic friction modifiers (OFMs), oil-soluble organic molybdenum additives, functional polymers, and nanoparticles. Owing to the excellent friction reduction effect of the molybdenum disulfide, some molybdenum compounds are widely used as precursors of molybdenum disulfide in engine lubricants. However, oil-soluble organomolybdenum compounds usually contain sulfur, phosphorus and metal elements,

which will increase the content of thermal oxidation deposits in the lubricating oil [10–13]. These deposits may accumulate in the channel of the particle filter, further damaging the three-way catalytic converter system of automobile exhaust emissions. The application of molybdenum-based FMs has been limited under the increasingly stringent environmental protection regulations and oil specification requirements. Meanwhile, nanoparticles and functional polymers cannot be widely used in a short time due to limitations from solubility and classification [14–19]. OFMs do not contain harmful and metallic elements, which can meet the requirements of environmental protection and energy conservation. Thus, they have application value in the development of future additives [9,20–30]. So far, reports on OFMs mainly focus on the performance comparison, formulation development and mechanism research of existing molecular structures. Additionally, there is a lack of systematic study on the structure-activity relationship between molecular structure and tribological properties. The purpose of the research is to investigate the synthesis and performance evaluation of a single lubricant additive, helping to develop OFMs for low viscosity engine oil and reduce the friction coefficient between the engine piston ring and cylinder liner.

Polyether amine is a kind of linear polymer formed by the diblock copolymerization of ethylene oxide (EO) and propylene oxide (PO), containing amine-based terminal active functional groups. Polyether amine has the properties of temperature-dependent phase separation, wide molecular weight range, repeated unit distribution and excellent low temperature performance [31]. The O and N atoms can provide multiple chelating sites to facilitate metal surface adsorption. More importantly, the molecular structure of polyether amine can be modified through different reactions to form various structures such as imines, amides and imine bonds (schiff bases), thus achieving versatile applications. In addition, as a widely used bulk chemical, low-cost polyether amines possess a great prospect in the field of lubrication additives through proper functionalization.

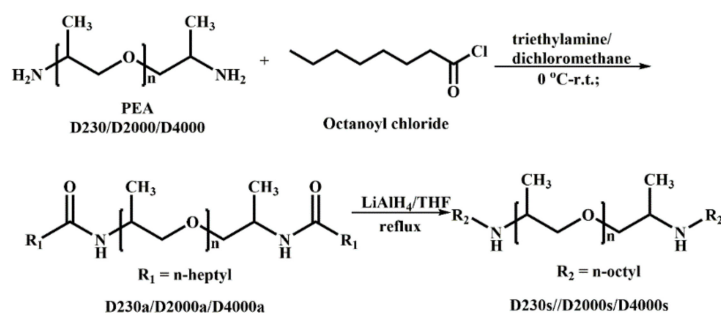
It is empirically known that the secondary amine derivatives obtained by alkylation of amino-PEG2-amine exhibit outstanding friction reduction and wear resistance properties [32]. In order to further expand the application of this type of compounds as OFMs, polyether amines (D230, D2000 and D4000) with different molecular weights were applied as precursors in this paper. The polyether amine derivatives were obtained by amidation and further reduction by lithium aluminium hydride ( $\text{LiAlH}_4$ ). The above polyether amine derivatives were added into PAO4 base oil as OFMs to investigate their tribological properties under different contact configurations. The influence of molecular weights on the properties of these compounds was discussed, with the lubrication mechanism of polyether amine alkylation derivatives explored through the surface analysis of wear marks. The frictional experiments were performed on a four-ball friction tester, point-on-flat and line-on-flat reciprocation friction tests. The wear scars were observed by scanning electron microscopy-energy dispersive spectrometry (SEM-EDS), three-dimensional (3D) profiler, and Raman spectra.

## 2. Materials and Methods

### 2.1. Reagents and Instruments

Octanoyl chloride (99.0%), Polyether amine D230, D2000 and D4000, triethylamine (TEA, 99.0%),  $\text{LiAlH}_4$  (97.0%) and tetrahydrofuran (THF, 99.5%) were purchased from Adamas Chemical Reagent Co., Ltd (Shanghai, China) and Energy Chemical Reagent Co., Ltd. (Shanghai, China). The synthetic route was listed in Scheme 1.

NMR spectra were carried out on a BRUKER AVANCE III HD spectrometer. Molecular weights were recorded with a Malvern GPC 305. IR data was recorded on PerkinElmer Spectrum Two FT-IR (ATR). The thermal stability was obtained on a TA-SDTQ600 instrument. The contact angle was obtained from a KRUSS surface tension meter. EDS data was recorded on an Octane Elect Plus. Raman spectroscopy was performed using a Thermo Fisher DXR.



**Scheme 1.** Synthetic scheme for alkylated derivatives of polyether amines (PEA).

## 2.2. Synthesis of D230s

In a 500 mL round-bottomed flask, polyether amine D230 (17.13 g), triethylamine (22.5 g) and dichloromethane (300 mL) were added. Then octyl chloride (24.2 g) was added to the flask via a drop funnel in an ice bath. The reaction was then continued at room temperature for 24 h. An appropriate amount of water was added to terminate the reaction and the organic phase was then separated and washed twice with deionized water. The organic phase was dried with anhydrous sodium sulfate and the amide product D230a was obtained by decompression and evaporation of the solvent (26 g, yield 72.4%).

Anhydrous THF (300 mL) in a round-bottom flask was cooled in an ice bath.  $\text{LiAlH}_4$  (1.6 g) and the intermediate product D230a (10 g) were then added in batches. After the addition, the reaction was refluxed under nitrogen protection for two days. Then a small amount of water was dropped to remove excessive reducing agent. After the bubbles were fully stirred, an appropriate amount of dichloromethane and anhydrous sodium sulfate were added. The solution was stirred until the solution was clear. Then the solvent was evaporated to obtain the polyether amine n-octyl substituted derivative D230s (6.8 g, yield 72.2%).

## 2.3. Synthesis of D2000s

D2000s was synthesized in a method analogous to D230s in 65.8% yield as a colorless oil.

## 2.4. Synthesis of D4000s

D4000s was synthesized in a method analogous to D230s in 58.8% yield as a yellow oil.

## 2.5. Infrared Spectra of Alkylation Derivatives of Polyether Amines

Figure 1 compares the IR spectra of polyether amines, amide products and alkylation derivatives with different molecular weights. The peaks around  $3300\text{--}3660\text{ cm}^{-1}$  correspond to the N-H bond, and the peaks around  $2800\text{ cm}^{-1}\text{--}2900\text{ cm}^{-1}$  correspond to  $\text{CH}_2/\text{CH}_3$ . The peaks around  $1460\text{ cm}^{-1}$  belong to the bending vibration of the C-H bond, and the peaks around  $1370\text{ cm}^{-1}$  is the bending vibration of the C-N bond. The peak near  $1110\text{ cm}^{-1}$  is the characteristic band of the polyether C-O-C bond. The obvious C=O peak (near  $1640\text{ cm}^{-1}$ ) can be seen in the IR spectra of the aminated derivatives, indicating that the amidation of polyether amine has been successfully carried out. In the IR spectra of alkylated derivatives, the C=O peak disappeared, and the N-H stretching vibration peak changed from a wide peak at  $3300\text{ cm}^{-1}$  to a narrow peak at  $3360\text{ cm}^{-1}$ , indicating that the amide derivatives were completely reduced and the alkylated derivatives were obtained. With the increase of the molecular weights of polyether amines, the proportion of amine group in the molecule decreased significantly, and therefore the C=O and N-H signals gradually weakened.

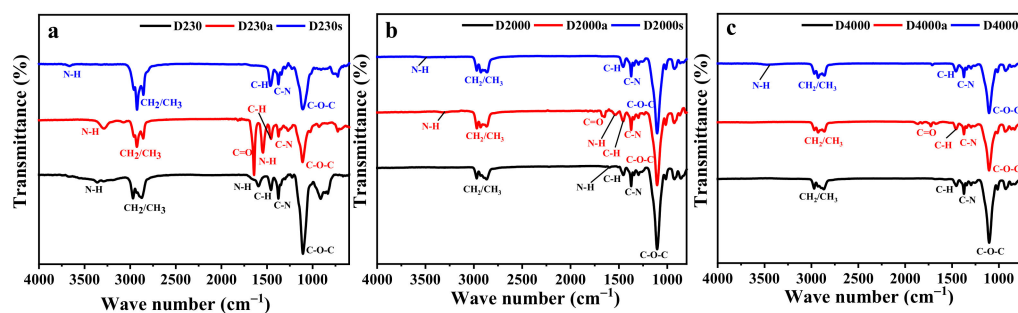


**Figure 1.** IR spectra of polyether amines and the corresponding derivatives with different molecular weights (a) D230, (b) D2000, (c) D4000. The black curves: polyether amines; the red curves: amide products of polyether amines; the blue curves: n-octyl substituted polyether amines).

### 2.6. NMR Spectra of Alkylation Derivatives of Polyether Amines

NMR spectra were applied to further verify the structures of the products. Figure 2a shows the  $^1\text{H}$  NMR and Figure 2b  $^{13}\text{C}$  NMR spectra of the alkylation derivatives of polyether amines.

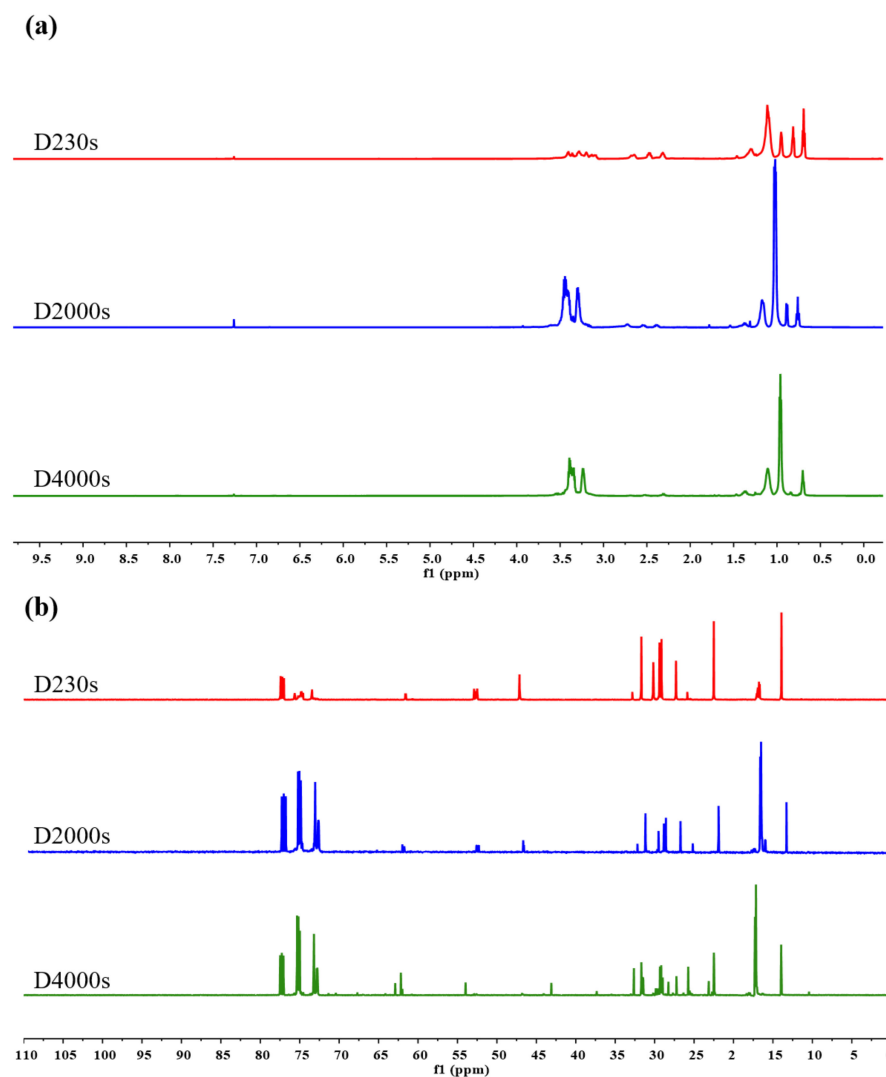


**Figure 2.**  $^1\text{H}$  NMR (a) and  $^{13}\text{C}$  NMR (b) of n-octyl substituted derivatives of polyether amines.

In the  $^1\text{H}$  NMR spectrum, the peak at 0.6 ppm–1.3 ppm represent  $-\text{CH}_3/-\text{CH}_2^-$ , and the peaks at 2.2 ppm–2.7 ppm represent  $-\text{CH}_2^-$  connected with NH. The peak intensity

here gradually decreases with the increase of molecular weight, resulting from the gradual decrease of the proportion of NH in the molecule. The peaks between 3.0 ppm and 3.5 ppm represent  $-\text{OCH}_2^-$ , and the peak displacement was found towards the low field for D2000s and D4000s. This may be because the oxygen-containing functional groups have an unshielding effect on the hydrogen on the  $-\text{CH}_2^-$  group. With the increase of oxygen-containing functional groups, the hydrogen displacement on  $-\text{OCH}_2^-$  gradually increases. Figure 2b illustrates the comparison results of  $^{13}\text{C}$  NMR, in which the peaks at 73 ppm–75 ppm represent  $-\text{OCH}_2^-$ , the peaks at 47 ppm and 52 ppm correspond to  $-\text{CH}_2^-$  associated with NH, and the peaks at 13 ppm–31 ppm correspond to  $-\text{CH}_3/-\text{CH}_2^-$ . It can be seen that  $-\text{CH}_2^-(\text{NH})$  gradually weakens with the increase in molecular weight, while the strength of  $-\text{OCH}_2^-$  increases significantly after the molecular weight exceeds 2000, resulting in the significant increase in the  $-\text{OCH}_2^-$  proportion.

### 2.7. Elemental Contents and Molecular Weights of Alkylation Derivatives of Polyether Amines

The contents of C, H, O and N of the three polyether amine alkylation derivatives were determined by elemental analysis. The results are shown in Table 1. It can be indicated that the content of N element gradually decreases with the increase of molecular weight. When the molecular weight increases to 2000, the nitrogen content of D2000s decreases by 77.4% in comparison to that of D230s. In addition, the increase of molecular weight makes the content of the oxygen element increase noticeably.

**Table 1.** Element contents of alkylation derivatives of polyether amines.

Sample	N (%)	O (%)	C (%)	H (%)
D230s	5.045	12.151	70.515	12.289
D2000s	1.140	26.484	62.250	10.126
D4000s	0.505	25.133	63.925	10.437

The molecular weights of the alkylation derivatives of polyether amines are listed in Table 2. It can be found that the molecular weights of the three polyether amine derivatives—D230s, D2000s, and D4000s, increased successively.

**Table 2.** Molecular weights of alkylation derivatives of polyether amines.

Sample	Mn (Daltons)	Mw (Daltons)	Mz (Daltons)	Mw/Mn
D230s	98	218	378	2.219
D2000s	485	1430	2342	2.948
D4000s	3486	5119	7321	1.468

### 2.8. Thermal Stability Analysis of the Alkylation Derivatives of Polyether Amines

Figure 3 shows the thermogravimetric curves of three alkylation derivatives of polyether amines with different molecular weights. The thermogravimetric curves indicate that molecular weight has a direct influence on the thermal stability of the alkylation derivatives of polyether amine. With the increase of molecular weight, the slope of thermal decomposition curve becomes low and the decomposition temperature increases. Among them, the initial decomposition temperature of D230s was about 190 °C, and the final decomposition temperature was 280 °C. The initial decomposition temperature of D2000s rose to 288 °C, and the final decomposition temperature was 390 °C, indicating that the thermal stability of D2000s was significantly improved. When the molecular weight of polyether amine continues to increase to 4000, its alkylated product D4000s experienced two short thermal weight losses below 220 °C and began to decompose at 332 °C, indicating that there was a small amount of low molecular weight polymer in D4000s. Overall, the thermal stabilities of D2000s and D4000s were close.

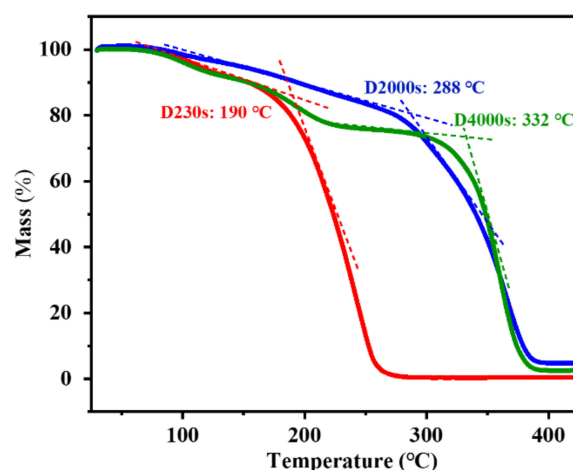


**Figure 3.** Thermo-gravimetric curves of alkylated derivatives of polyether amines.

### 2.9. Tribological Test Conditions

In this work, the friction reduction and wear resistance performance of polyether amine alkylation derivatives as OFMs were evaluated under three different friction contact modes of point-to-point, point-on-flat and line-on-flat, respectively. The friction pair materials used in the friction experiment were GCr15 steel and the temperature was room temperature. The selected GCr15 steel has excellent hardness and wear resistance, which is widely used in the tribological performance evaluation of lubrication additives. Properties of the base oil are shown in Table 3.

**Table 3.** Physical and chemical properties of PAO4.

Parameter	Value
Flash point (°C)	220
Pour point (°C)	−66
density (g/ml, 25 °C)	0.815
Kinematic viscosity @40 °C (mm <sup>2</sup> /s)	19.0
Kinematic viscosity @100 °C (mm <sup>2</sup> /s)	4.1
Viscosity index	117

The addition amount was 0.5 wt%. The procedure used for the dissolution of the additives in the base oil is as follows: A certain amount of polyether amine derivative was added to the base oil and stirred at 60 °C for 30 min. The transparent mixture was then cooled to room temperature for friction tests. Specific friction test conditions are as follows: four-ball friction experimental conditions (point-to-point contact): load, 196 N (~5.3 GPa initial maximum Hertzian contact pressure); rotating speed, 1200 rpm; temperature at room temperature; time, 30 min; diameter of ball (GCr 15 steel), 12.7 mm. The schematic diagram of the friction mode is shown in Figure 4a. UMT reciprocating friction test conditions (point-on-flat contact): the ball of GCr 15 steel (diameter 8 mm) was used for point-on-flat reciprocating friction with a fixed frequency of 2 Hz relative to the fixed steel plate (GCr15 steel). The load was 7 N (~1.0 GPa initial maximum Hertzian contact pressure), and the stroke was 10 mm. The schematic diagram of the friction mode is shown in Figure 4b.

The friction diagram of line-on-flat (160 N, ~350 MPa initial maximum Hertzian contact pressure) is shown in Figure S1. All the friction tests were carried out at least twice in each group to ensure repeatability.

The steel balls after point-to-point friction tests and the steel plate after point-on-flat and line-on-flat friction tests were washed twice with petroleum ether, and the three-dimensional morphology of the worn surfaces were observed through a white light interferometry.

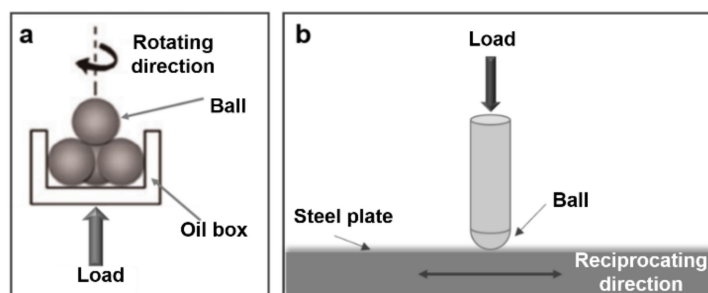


Figure 4. Schematic diagram: (a) point-to-point contact mode, (b) UMT point-on-flat contact mode.

### 3. Results

#### 3.1. Tribological Properties of Point-to-Point Contact on Four-Ball Friction Tester

The tribological properties of the three polyether amine alkylation derivatives under point-to-point contact configuration were investigated on a four-ball friction and wear tester. Figure 5 compares the wear scar diameters and friction coefficients lubricated by liquids with and without polyether amine alkylation derivatives. It can be found that the alkylation derivatives of polyether amine showed no friction reduction properties, but obvious wear resistance properties. Specifically, under the lubrication of the base oil, the average wear scar diameter on the steel balls was 0.490 mm. The addition of polyether amine alkylation derivatives reduced the wear scar diameter noticeably. Among them, D2000s showed the best anti-wear performance with an average wear scar diameter of 0.390 mm (reduced by 20.4% compared with the base oil). In contrast, D230s and D4000s decreased the wear scar diameter by 17.7% and 17.6%, respectively.

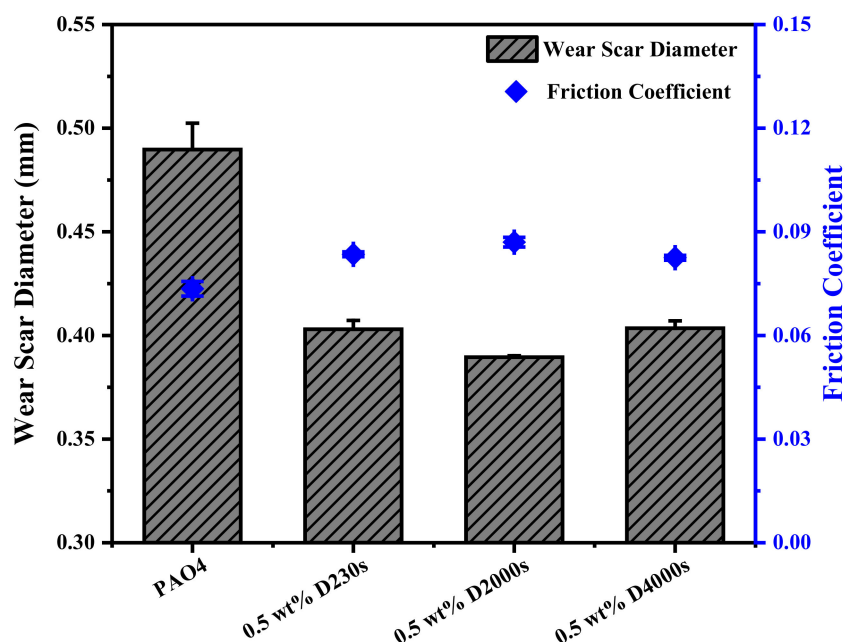
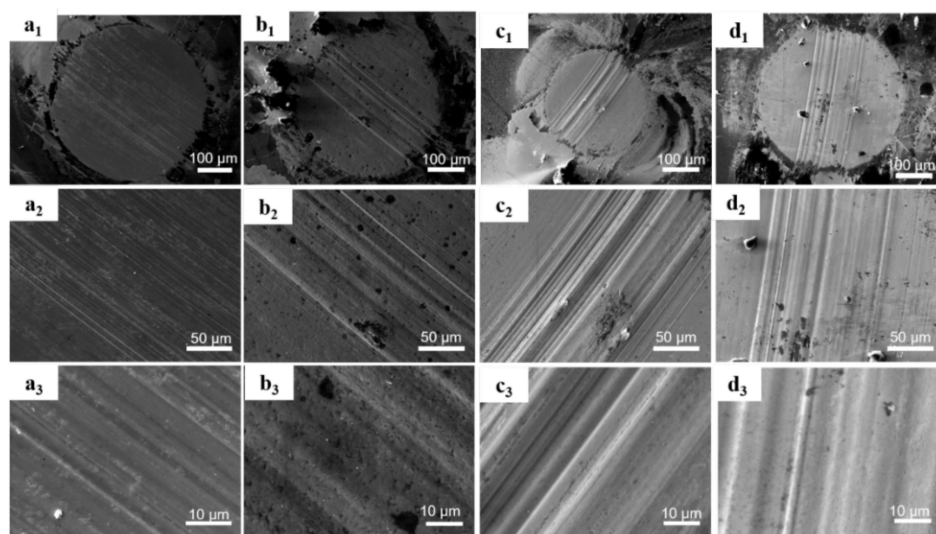


Figure 5. Wear scar diameters and friction coefficients for four-ball friction tests.

SEM was used to analyze the surface morphology of the steel balls (Figure 6). It can be found that dense scratches appeared on the surface of the ball lubricated with the neat base oil. With the addition of polyether amine alkylation derivatives, the diameter of the wear scar decreased, and the scratches on the spot became sparse, located mainly in the middle area. The surface lubricated with oil containing D230s showed lots of small pits. With the increase of additive molecular weight, the wear marks became gradually smooth. The surface texture of the wear spot lubricated by oil containing D4000s was relatively shallow,

while the spot diameter was larger than that of D2000s. Consequently, the SEM morphology evaluation showed that D2000s exhibited the best wear resistance performance.



**Figure 6.** Comparison of wear scar morphology in four-ball friction tests (a<sub>1</sub>/a<sub>2</sub>/a<sub>3</sub>: PAO4; b<sub>1</sub>/b<sub>2</sub>/b<sub>3</sub>: 0.5 wt% D230s; c<sub>1</sub>/c<sub>2</sub>/c<sub>3</sub>: 0.5 wt% D2000s; d<sub>1</sub>/d<sub>2</sub>/d<sub>3</sub>: 0.5 wt% D4000s).

### 3.2. Tribological Properties of Point-on-Flat Contact on UMT Friction Tester

Figure 7 compares the friction coefficients of polyether amine alkylated derivatives under UMT point-on-flat friction tests. Compared with the base oil (with an average friction coefficient of 0.164), adding 0.5 wt% polyether amine derivatives with different molecular weights can improve the friction reducing performance to a different extent (0.159–0.145). The friction coefficient of lubricant with D2000s was 0.145, which was 11.6% lower than that of the base oil. When the molecular weight increased to 4000, the friction coefficient increased slightly.

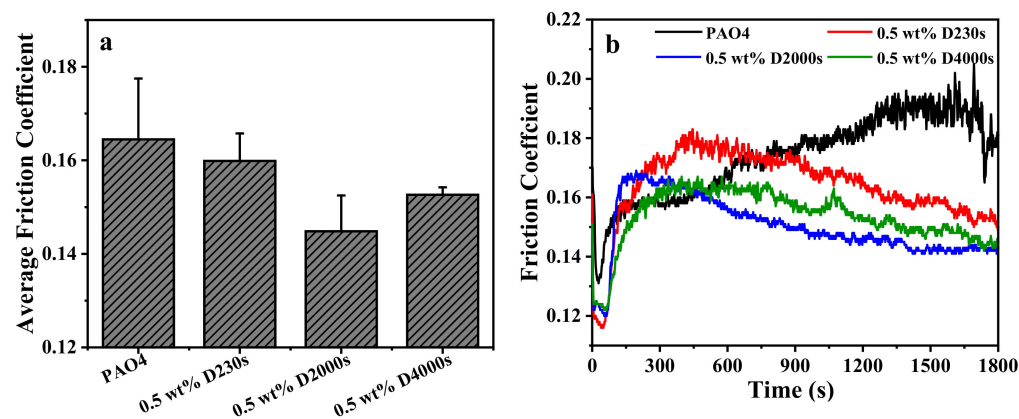


**Figure 7.** Average friction coefficients (a) and friction coefficient curves (b) for UMT point-on-flat friction tests.

As can be seen from the friction coefficient curve in Figure 7b, the friction coefficient of the base oil showed a trend of gradual increase, while the friction coefficient of the lubricants with polyether amine alkylation derivatives gradually decreased. The friction coefficient curve of D2000s was smoother and lower than that of the other two molecular weight derivatives.

White light interferometry was applied to measure the wear volume of the upper steel balls and calculate the wear rates. The wear rates and three-dimensional morphology are

shown in Figures 8 and 9, respectively. The results show that D230s can reduce the wear rate of the base oil by 11.8%. With the increase of molecular weight, D2000s can reduce the wear rate of base oil by 50.4%. When the molecular weight continues to increase to 4000, the wear rate increased relative to D2000s, and decreased by 10.2% relative to the base oil. It can be indicated that D2000s showed better anti-wear performance compared with the other two polymers in the point-on-flat friction experiments.

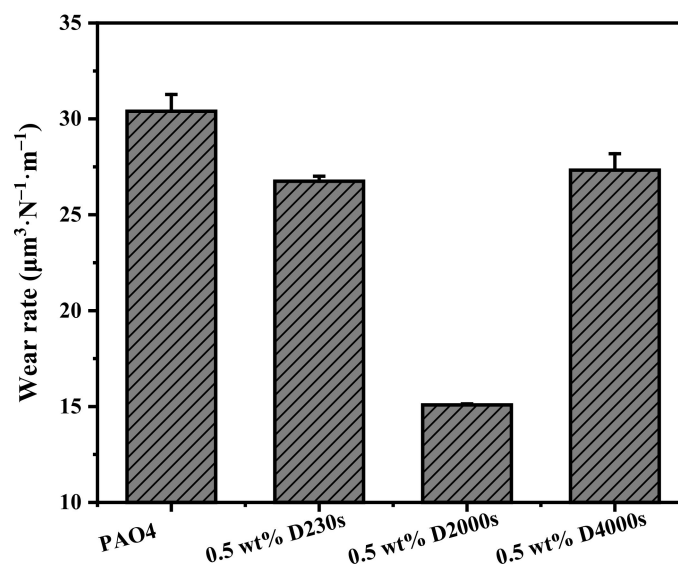


Figure 8. Wear rates of steel balls after UMT point-on-flat friction tests.

As shown in Figure 9, the surface wear mark width of the steel ball lubricated with base oil is 0.372 mm, and the addition of polyether amine alkylation derivatives can reduce the wear mark width to 0.246–0.341 mm, with an average wear mark depth of 1.991–2.353  $\mu\text{m}$ . The width and depth of wear marks on the ball surface lubricated by D2000s oil were the smallest, which are similar to the reduction in friction coefficient.

The tribological properties of line-on-flat contact on TE77 friction tester can be found in the Supplementary Materials.

In summary, the prepared polyether amine alkylation derivatives showed remarkable wear resistance under different friction modes, while they exhibited friction reducing properties under relatively mild point-on-flat and line-on-flat contact modes. Polyether amine alkylation derivatives are a class of linear polymers, the active adsorption sites of which are located on the main chain of polyether amines. When the derivatives were used as OFMs, the molecules can be adsorbed onto the metal surface along the main chain, forming the form of “pancake” or “brush” [33]. It has been reported that these adsorbed polymers can be very effective in reducing friction at relatively mild rolling/sliding friction, but less effective under harsh lubrication conditions [34,35]. Point-to-point contact mode is a kind of relatively harsh condition (with an actual contact pressure of  $\sim 5.3$  GPa), while the contact pressure of the point-on-flat and line-on-flat contact mode are 1.0 GPa and 350 MPa, respectively. Thus, polyether amine alkylated derivatives in the relatively mild friction condition showed an obvious anti-friction effect.

Unlike small molecule OFMs, when polymer molecules are adsorbed on the metal surface, they will spatially hinder the adsorption of other polymer molecules in the system. The increase in molecular weight means that the polymer OFMs adsorbed on the metal surface resembles a “mushroom” rather than a “pancake” or “brush” [21]. The increase of polymer molecular weight can increase the number of active adsorption sites and further improve the adsorption strength and surface coverage of additive molecules on the metal surface. On the other hand, it can be hypothesized that some molecules may have difficulty in reaching the surface for a reaction to take place because of the steric hindrance, leading to the lower coverage and the decrease of tribological properties [33]. When the molecular

weights of polyether amines increased from 230 to 2000, the antifriction properties of its derivatives as OFMs were significantly improved, while the antifriction properties did not further improve when the molecular weight continued to increase to 4000. This indicates that with the increase of polymer molecular weight, the number of O atoms as the adsorption sites in the molecule increases, which promotes the adsorption of polymer molecules on the friction surface. On the other hand, an increase in steric hindrance due to an increase in molecular weight is not conducive to the close accumulation of additive molecules on the friction surface. As such, excessive molecular weight will not improve the friction reduction and anti-wear performance.

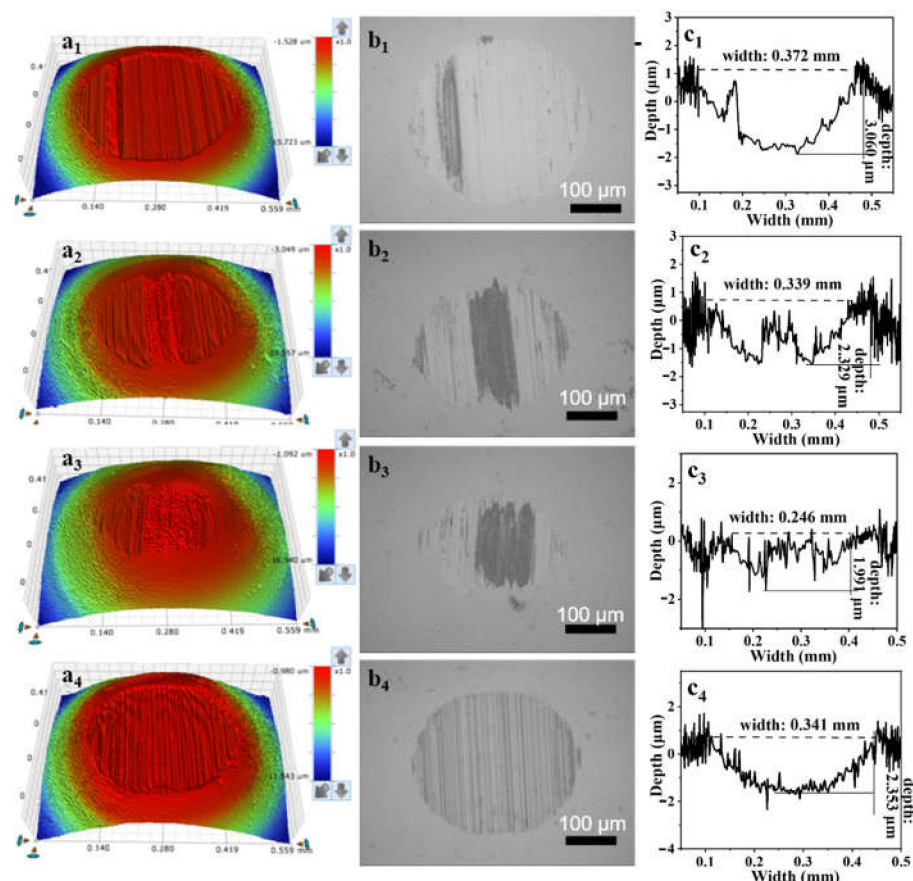


**Figure 9.** Three-dimensional shape, micrographs and size of wear marks of steel balls after UMT point-on-flat friction tests ( $a_1/b_1/c_1$ : PAO4,  $a_2/b_2/c_2$ : D230s in PAO4,  $a_3/b_3/c_3$ : D2000s in PAO4,  $a_4/b_4/c_4$ : D4000s in PAO4).

### 3.3. Adsorption Mechanism

To investigate the adsorption mechanism of polyether amine derivatives as OFMs, the addition concentration was increased to 2.0 wt% for water contact angles measurement of the steel surfaces. When the concentration of polyether amine derivatives increased to 2.0 wt%, the antifriction performance trend was consistent with that mentioned above (Figure S4). Water contact angles were measured to estimate the adsorption ability of the polar additives on the steel surfaces (Figure 10). The dipping and rinsing process involved submerging a steel plate in the lubricant with or without polymer molecules for 2 h at r.t. After that, the oil on the steel plate was washed with toluene and then dried in air. The contact angle of the steel plate surface was then tested. It can be seen from the result that the addition of the polyether amine derivatives led to the reduction of contact angles of the steel surfaces, which indicated that the polarity of the surfaces had increased. Specifically, the contact angle of the surfaces treated with different polyether amine derivatives decreased with varying degrees ( $70.36^\circ$ – $82.48^\circ$ ). The contact angle of the surface treated by D2000s

was the lowest among the three additives ( $70.36^\circ$ ), indicating that the amount of adsorption was the largest among the three additives. The contact angles of the surfaces treated by D230s and D4000s were  $82.48^\circ$  and  $75.62^\circ$ , respectively. From the perspective of the change trend of the contact angles, it gradually decreased and then slightly increased as the molecular weight of the polyether amine derivative increased. It can be hypothesized that the alkylated polyether amine derivatives as lubricating additives can be adsorbed on the surface of the steel to different degrees. Additionally, the molecular weight will affect its adsorption capacity, and the derivative with a molecular weight of 2000 exhibited superior adsorption performance.

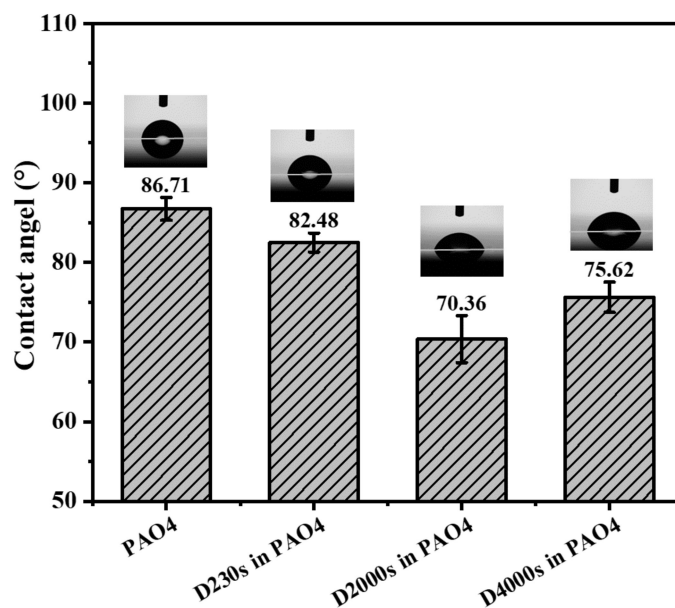


**Figure 10.** Aqueous contact angles on the steel plates dip-coated with the lubricants with and without polyamine derivatives.

### 3.4. Analysis of the Worn Surfaces after Point-to-Point Friction Tests

To investigate the information of the worn surfaces by EDS, the addition concentration was also increased to 2.0 wt%. EDS was used to analyze the elements of the steel ball spots after four-ball friction tests. Laser confocal Raman was used to further analyze the components.

#### 3.4.1. EDS Analysis

After the four-ball friction tests, brown deposits were formed in the abrasive spot and its edge. Table 4 and Figure 11 show the EDS energy spectrum comparison of the abrasive spots and their edge deposits.

**Table 4.** Comparison of element content in the surface and the edge of the grinding spots.

Element	PAO4 (%)		D230s in PAO4 (%)		D2000s in PAO4 (%)		D4000s in PAO4 (%)	
	surface	edge	surface	edge	surface	edge	surface	edge
C	1.0	22.8	1.4	13.6	1.0	18.4	1.0	12.9
O	0.3	1.1	0.4	4.3	0.0	10.5	0.2	3.0
Fe	97.1	74.7	96.9	80.8	97.5	70.0	97.1	82.5
Cr	1.3	1.2	1.4	1.1	1.5	0.9	1.3	1.2
Mn	0.3	0.2	0.0	0.3	0.00	0.0	0.4	0.4

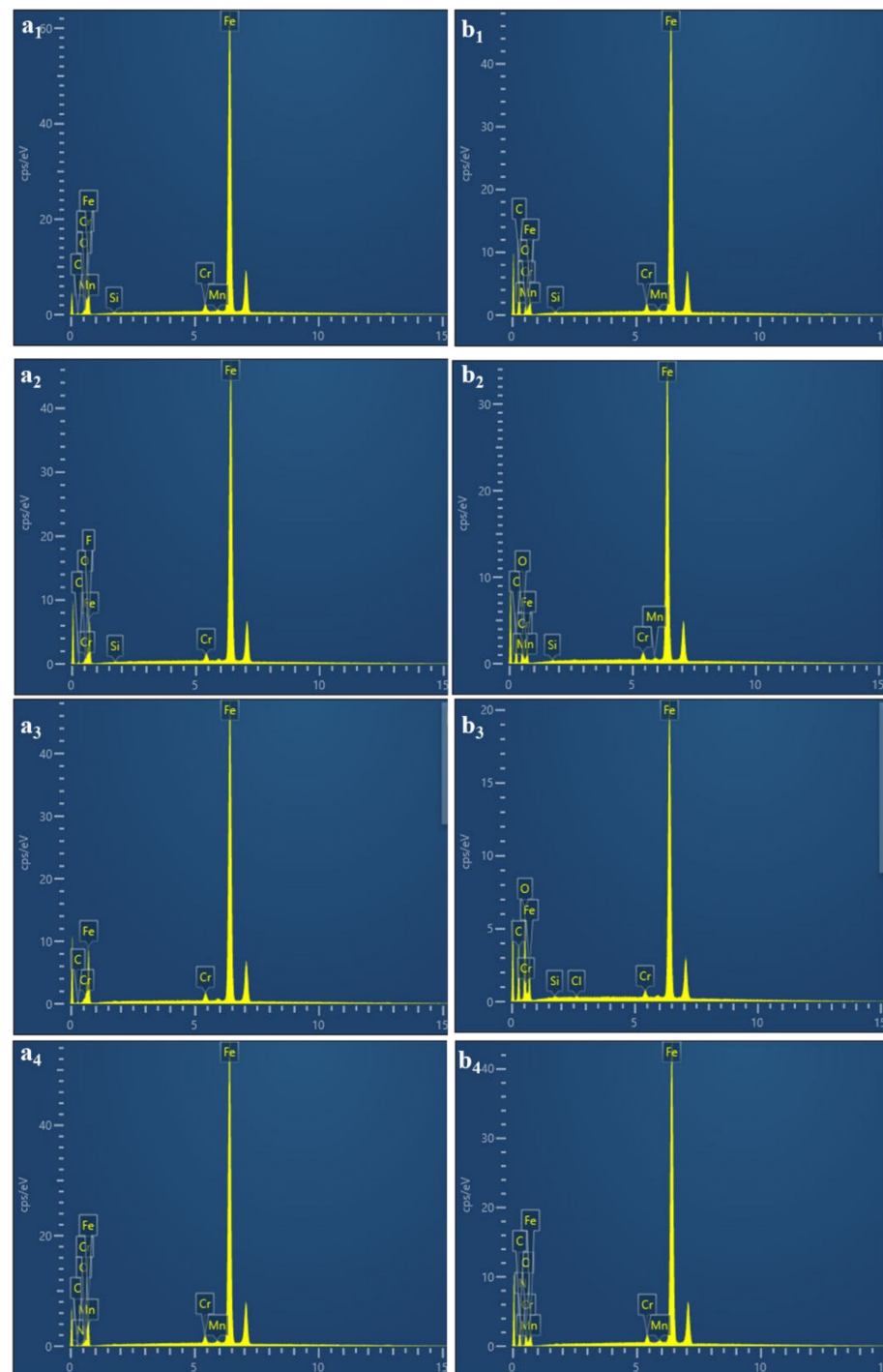


**Figure 11.** Comparison of the EDS energy spectra of the deposits at the grinding spots and their edges (a<sub>1</sub>/b<sub>1</sub>: PAO4; a<sub>2</sub>/b<sub>2</sub>: D230s in PAO4; a<sub>3</sub>/b<sub>3</sub>: D2000s in PAO4; a<sub>4</sub>/b<sub>4</sub>: D4000s in PAO4).

The results show that sediments are dominated by Fe, C and O elements, indicating that the main adsorption sites of polyether amine alkylation derivatives as OFMs are O atoms. The polymer molecules are first adsorbed on the metal surface by the O atoms, and the tribochemical reaction occurs to form a lubricating protective film on the friction surfaces under the shear action of the friction pair. EDS element content comparison showed that the element content at the edge of the spot was higher than that of the spot surface, indicating that the protective film was easy to be sheared and deposited around the spot during the tests. In addition, the content of O element on the worn surface lubricated

by the oil containing polyether amine alkylation derivatives was relatively high, which indicated that polyether amine derivatives can promote the formation of tribochemical film, thus reducing friction and wear.

### 3.4.2. Raman Analysis

Johnson et al. [36] found that carbon film which has a lubricating effect was generated from hydrocarbon lubricating oil containing a cyclopropanoic acid (CPCA) additive after friction tests. The optical microscope and SEM test showed that the carbon film was generated near the contact area with high roughness and then filled to the rough surface. The carbon film was also sheared in the direction of sliding. Raman spectroscopy confirmed that this kind of carbon tribofilm was composed of a relatively soft amorphous graphite material. The additive molecules can form an effective and friction-induced carbon tribofilm at the friction interfaces without the catalyst. Wu et al. [37] further found that the lubricant added with CPCA could generate a frictional film with anti-wear protection without any surface pretreatment. Raman spectra show that the tribofilms have D and G peaks, similarly to those of graphite or DLC films. Further friction experiments and molecular dynamics simulations showed that these tribofilms were high molecular weight hydrocarbon polymers that can be used as solid lubricants.

According to the mechanism analysis results of the above studies, Raman spectroscopy was used in this paper to analyze the sediment composition on the surface of the wear mark after point-to-point friction tests. Figure 12 shows the Raman spectrum of the surfaces of the wear mark excited by a 532 nm laser. The peaks near  $403\text{ cm}^{-1}$ ,  $290\text{ cm}^{-1}$  and  $223\text{ cm}^{-1}$  represent  $\alpha\text{-Fe}_2\text{O}_3$  [38], and the peak near  $665\text{ cm}^{-1}$  is  $\text{Fe}_3\text{O}_4$  [39]. The peaks near  $1322\text{ cm}^{-1}$  and  $1580\text{ cm}^{-1}$  correspond to the D peak and G peak of carbon materials, respectively. A  $2900\text{ cm}^{-1}$  peak corresponds to a 2D peak. Among them, the 2D peaks signal of D2000s and D4000s are slightly stronger. Raman spectra showed that carbon films with a lubrication function were formed. The alkylation derivatives of polyether amines adsorbed on the friction surface were beneficial to the formation of tribochemical film. When the micro bulges on the metal surface are in direct contact with each other, the instantaneous high temperature and high pressure may cause the decomposition of the compounds and eventually form the carbon friction film. This kind of friction film is soft, and the fragments formed by shearing can fill the metal surface, thus reducing the roughness and improving the tribological properties of the oil.

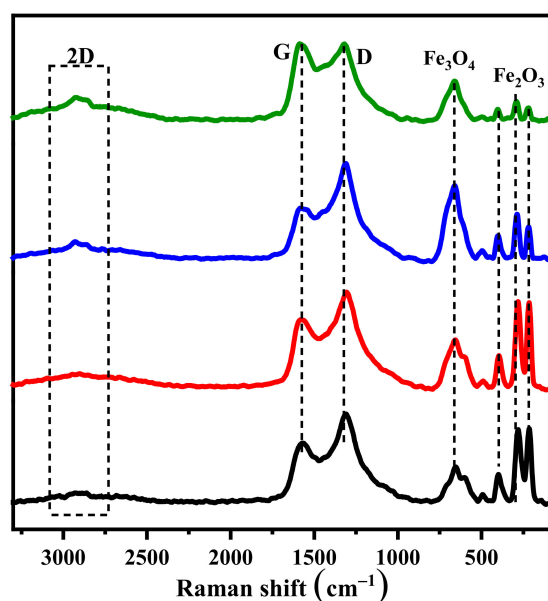


**Figure 12.** Raman spectra of deposits at steel ball wear spots (black: PAO4; red: D230s in PAO4; blue: D2000s in PAO4; green: D4000s in PAO4).

#### 4. Conclusions

Three derivatives were obtained by the alkylation of polyether amines with different molecular weights through acylation and reduction reactions. The friction tests under different working conditions were designed to investigate the antiwear properties of polyether amines. The compositions of the worn surfaces were analyzed and the lubrication mechanism of the additive was explored. The present work can provide a theoretical and experimental basis for developing a friction modifier suitable for low viscosity engine oil. Through the work of this paper, we can draw the following conclusions:

- (1) Polyether amine alkylated derivatives as OFMs exhibit obvious wear resistance in point-to-point, point-on-flat and line-on-flat contact modes, and perform well in relatively mild point-on-flat and line-on-flat friction tests. Among them, D2000s showed a superior anti-friction effect.
- (2) The lone pair electrons on the oxygen atom can form coordination bonds with the vacant *d* orbital on the metal surface. The intermolecular hydrogen bonds are also helpful for the molecular association of the additive to form a dense adsorption film on the metal surface. The increase of molecular weights of the polymers makes the number of active adsorption sites increase, which is beneficial to the improvement of tribological properties. However, once the molecular weight increases to a certain extent, it is not conducive to the formation of adsorption film.
- (3) The surface morphology and composition analysis show that the lubricating films are mainly carbon films and iron oxides. Polyether amine alkylated derivatives are a kind of linear polymers. The molecules are arranged on the metal surfaces along the polar parts of the main chains, which are further transformed into carbon friction films through an in situ tribochemical reaction. Fragments formed by carbon film under the shear action of friction pairs fill the rough surfaces and then reduce the surface roughness. Given that the formation rate is greater than the wear removal rate, the friction film is effective in reducing friction and wear. The carbon film avoids direct contact of the sliding surfaces, thus significantly improving the tribological properties.

**Supplementary Materials:** The following supporting information can be downloaded at: <https://www.mdpi.com/article/10.3390/lubricants10060105/s1>, TE77 reciprocating friction test conditions (line-on-flat contact) (Page S1); The friction diagram of line-on-flat (Figure S1); The tribological properties of line-on-flat contact on TE77 friction tester (Page S2–S3); Friction coefficient curves for UMT point-on-flat friction tests at the concentration of 2.0 wt% (Figure S4).

**Author Contributions:** Conceptualization, W.H. and J.L.; methodology, W.H. and J.L.; validation, W.H. and J.L.; formal analysis, W.H. and J.L.; investigation, W.H.; data curation, W.H. and J.L.; writing—original draft preparation, W.H.; writing—review and editing, J.L.; supervision, J.L. All authors have read and agreed to the published version of the manuscript.

**Funding:** The authors would like to thank the financial support for this work by “Youth Innovation Promotion Association, CAS (2019288); Shanghai Pudong New Area Science and Technology Development Fund (PKJ2019-C01) and Strategic Priority Research Program of the Chinese Academy of Sciences (XDA21021202)”.

**Institutional Review Board Statement:** Not applicable.

**Informed Consent Statement:** Not applicable.

**Data Availability Statement:** Not applicable.

**Conflicts of Interest:** The authors declare that they have no known competing financial interests or personal relationships that could influence the work reported in this paper.

## References

1. Holmberg, K.; Erdemir, A. Influence of tribology on global energy consumption, costs and emissions. *Friction* **2017**, *5*, 263–284. [[CrossRef](#)]
2. Holmberg, K.; Andersson, P.; Erdemir, A. Global energy consumption due to friction in passenger cars. *Tribol. Int.* **2012**, *47*, 221–234. [[CrossRef](#)]
3. Wong, V.W.; Tung, S.C. Overview of automotive engine friction and reduction trends—Effects of surface, material, and lubricant-additive technologies. *Friction* **2016**, *4*, 1–28. [[CrossRef](#)]
4. Tanaka, H.; Nagashima, T.; Sato, T.; Kawauchi, S. *The Effect of 0W-20 Low Viscosity Engine Oil on Fuel Economy*; SAE Technical Paper; SAE: Warrendale, PA, USA, 1999.
5. Singh, S.; Singh, S.; Sehgal, A. *Impact of low Viscosity Engine Oil on Performance, Fuel Economy and Emissions of Light Duty Diesel Engine*; SAE Technical Paper 2016-01-2316; SAE: Warrendale, PA, USA, 2016; p. 6.
6. Okuyama, Y.; Shimokoji, D.; Sakurai, T.; Maruyama, M. *Study of Low-Viscosity Engine Oil on Fuel Economy and Engine Reliability*; SAE Technical Paper 2011-01-1247; SAE: Warrendale, PA, USA, 2011; p. 9.
7. Tang, Z.; Li, S. A review of recent developments of friction modifiers for liquid lubricants (2007–present). *Curr. Opin. Solid State Mater. Sci.* **2014**, *18*, 119–139. [[CrossRef](#)]
8. Speight, J.G. *Lubricant Additives-Chemistry and Applications*, 2nd ed.; CRC Press: Boca Raton, FL, USA, 2009.
9. Spikes, H. Friction modifier additives. *Tribol. Lett.* **2015**, *60*, 5. [[CrossRef](#)]
10. Grossiord, C.; Varlot, K.; Martin, J.M.; Le Mogne, T.; Esnouf, C.; Inoue, K. MoS<sub>2</sub>, single sheet lubrication by molybdenum dithiocarbamate. *Tribol. Int.* **1998**, *31*, 737–743. [[CrossRef](#)]
11. Bec, S.; Tonck, A.; Georges, J.M.; Roper, G.W. Synergistic effects of MoDTC and ZDTP on frictional behaviour of tribofilms at the nanometer scale. *Tribol. Lett.* **2004**, *17*, 797–809. [[CrossRef](#)]
12. Morina, A.; Neville, A.; Priest, M.; Green, J.H. ZDDP and MoDTC interactions and their effect on tribological performance—Tribofilm characteristics and its evolution. *Tribol. Lett.* **2006**, *24*, 243–256. [[CrossRef](#)]
13. Laine, E.; Olver, A.V.; Lekstrom, M.F.; Shollock, B.A.; Beveridge, T.A.; Hua, D.Y. The effect of a friction modifier additive on micropitting. *Tribol. Trans.* **2009**, *52*, 526–533. [[CrossRef](#)]
14. Müller, M.; Topolovec-Miklozic, K.; Dardin, A.; Spikes, H.A. The design of boundary film-forming PMA viscosity modifiers. *Tribol. Trans.* **2006**, *49*, 225–232. [[CrossRef](#)]
15. Aoki, S.; Yamada, Y.; Fukada, D.; Suzuki, A.; Masuko, M. Verification of the advantages in friction-reducing performance of organic polymers having multiple adsorption sites. *Tribol. Int.* **2013**, *59*, 57–66. [[CrossRef](#)]
16. Qiu, S.; Dong, J.; Cheng, G. A review of ultrafine particles as antiwear additives and friction modifiers in lubricating oils. *Lubr. Sci.* **1999**, *11*, 217–226.
17. Bakunin, V.N.; Suslov, A.Y.; Kuzmina, G.N.; Parenago, O.P. Recent achievements in the synthesis and application of inorganic nanoparticles as lubricant components. *J. Nanopart. Res.* **2004**, *6*, 273–284. [[CrossRef](#)]
18. Sankaranarayanan, V.; Ramaprabhu, S. Graphene-based engine oil nanofluids for tribological applications. *ACS Appl. Mater. Inter.* **2011**, *3*, 4221–4227.
19. Wang, W.; Zhang, G.; Xie, G. Ultralow concentration of graphene oxide nanosheets as oil-based lubricant additives. *Appl. Surf. Sci.* **2019**, *498*, 143683. [[CrossRef](#)]
20. Onumata, Y.; Zhao, H.; Wang, C.; Morina, A.; Neville, A. Interactive effect between organic friction modifiers and additives on friction at metal pushing V-Belt CVT components. *Tribol. Trans.* **2017**, *61*, 474–481. [[CrossRef](#)]
21. Soltanahmadi, S.; Esfahani, E.A.; Nedelcu, I.; Morina, A.; van Eijk, M.C.P.; Neville, A. Surface reaction films from amine-based organic friction modifiers and their influence on surface fatigue and friction. *Tribol. Lett.* **2019**, *67*, 80. [[CrossRef](#)]
22. Zachariah, Z.; Nalam, P.C.; Ravindra, A.; Raju, A.; Mohanlal, A.; Wang, K.; Castillo, R.V.; Espinosa-Marzal, R.M. Correlation between the adsorption and the nanotribological performance of fatty acid-based organic friction modifiers on stainless steel. *Tribol. Lett.* **2019**, *68*, 11. [[CrossRef](#)]
23. Fry, B.M.; Moody, G.; Spikes, H.; Wong, J.S.S. Effect of surface cleaning on performance of organic friction modifiers. *Tribol. Trans.* **2019**, *63*, 305–313. [[CrossRef](#)]
24. Mitchell, K.; Neville, A.; Walker, G.M.; Sutton, M.R.; Cayre, O.J. Synthesis and tribological testing of poly(methyl methacrylate) particles containing encapsulated organic friction modifier. *Tribol. Int.* **2018**, *124*, 124–133. [[CrossRef](#)]
25. Shi, J.; Zhou, Q.; Sun, K.; Liu, G.; Zhou, F. Understanding adsorption behaviors of organic friction modifiers on hydroxylated SiO<sub>2</sub> (001) surfaces: Effects of molecular polarity and temperature. *Langmuir* **2020**, *36*, 8543–8553. [[CrossRef](#)]
26. Zhang, X.; Tsukamoto, M.; Zhang, H.; Mitsuya, Y.; Itoh, S.; Fukuzawa, K. Experimental study of application of molecules with a cyclic head group containing a free radical as organic friction modifiers. *J. Adv. Mech. Des. Syst.* **2020**, *14*, Jamdsm0044. [[CrossRef](#)]
27. Cyriac, F.; Tee, X.Y.; Poornachary, S.K.; Chow, P.S. Influence of structural factors on the tribological performance of organic friction modifiers. *Friction* **2021**, *9*, 380–400. [[CrossRef](#)]
28. Pominov, A.; Mueller-Hillebrand, J.; Traeg, J.; Zahn, D. Interaction models and molecular simulation systems of steel-organic friction modifier interfaces. *Tribol. Lett.* **2021**, *69*, 14. [[CrossRef](#)]
29. Li, W.; Kumara, C.; Meyer, H.M.; Luo, H.; Qu, J. Compatibility between various ionic liquids and an organic friction modifier as lubricant additives. *Langmuir* **2018**, *34*, 10711–10720. [[CrossRef](#)]

30. Kuwahara, T.; Romero, P.A.; Makowski, S.; Weihnacht, V.; Moras, G.; Moseler, M. Mechano-chemical decomposition of organic friction modifiers with multiple reactive centres induces superlubricity of ta-C. *Nat. Commun.* **2019**, *10*, 151–161. [[CrossRef](#)]
31. Xu, S.; Ye, L. Synthesis and properties of monomer cast nylon-6-b-polyether amine copolymers with different structures. *RSC Adv.* **2015**, *5*, 32460–32468. [[CrossRef](#)]
32. Hu, W.J.; Zhang, Z.J.; Zeng, X.Q.; Li, J.S. Correlation between the degree of alkylation and tribological properties of amino-PEG2-amine-based organic friction modifiers. *Ind. Eng. Chem. Res.* **2019**, *59*, 215–225. [[CrossRef](#)]
33. Brittain, W.J.; Minko, S. A structural definition of polymer brushes. *J. Polym. Sci. A Polym. Chem.* **2007**, *45*, 3505–3512. [[CrossRef](#)]
34. Smeeth, M.; Gunsel, S.; Spikes, H.A. *Friction and Wear Reduction by Boundary Film-Forming Viscosity Index Improvers*; SAE Technical Paper; SAE: Warrendale, PA, USA, 1996; p. 962037.
35. Muller, M.; Fan, J.; Spikes, H.A. Design of functionalized PAMA viscosity modifiers to reduce friction and wear in lubricating oils. *ASTM Int.* **2007**, *4*, JAI100956. [[CrossRef](#)]
36. Johnson, B.; Wu, H.; Desanker, M.; Pickens, D.; Chung, Y.W.; Wang, Q.J. Direct formation of lubricious and wear-protective carbon films from phosphorus- and sulfur-free oil-soluble additives. *Tribol. Lett.* **2018**, *66*, 2. [[CrossRef](#)]
37. Wu, H.; Khan, A.M.; Johnson, B.; Sasikumar, K.; Chung, Y.W.; Wang, Q.J. Formation and nature of carbon-containing tribofilms. *ACS Appl. Mater. Inter.* **2019**, *11*, 16139–16146. [[CrossRef](#)] [[PubMed](#)]
38. De Faria, D.L.A.; Venancio Silva, S.; de Oliveira, M.T. Raman microspectroscopy of some iron oxides and oxyhydroxides. *J. Raman Spectrosc.* **1997**, *28*, 873–878. [[CrossRef](#)]
39. Shebanova, O.N.; Lazor, P. Raman study of magnetite (Fe<sub>3</sub>O<sub>4</sub>): Laser-induced thermal effects and oxidation. *J. Raman Spectrosc.* **2003**, *34*, 845–852. [[CrossRef](#)]